

Wire tension in high-speed wire electrical discharge machining

Shi Wentai¹ · Liu Zhidong¹ · Qiu Mingbong¹ ·
Tian Zongjun¹

Received: 19 January 2015 / Accepted: 19 May 2015 / Published online: 11 June 2015
© Springer-Verlag London 2015

Abstract This paper investigated the wire tension change in high-speed wire electrical discharge machining (HSWEDM). The symmetry of the wire-winding mechanism and the resistance to the wire electrode on the upper and lower guide frames were considered the main causes of a non-even wire tension. Combined with the simulation model and the redesigned wire-winding mechanism, the adjusting wheel and the protection block were used to control the symmetry of the wire-winding mechanism and the resistance to the wire electrode on the upper guide frame. The wire tension was found to be capable of remaining stable in the machining process. The redesigned wire-winding mechanism can improve cutting stability and efficiency in large thickness cutting processes as well as the consistency of workpiece dimension in multi-cutting processes.

Keywords HSWEDM · Wire tension · Large thickness cutting · Multi-cutting

1 Introduction

Wire electrical discharge machining (WEDM) is a non-traditional process for machining various difficult-cutting

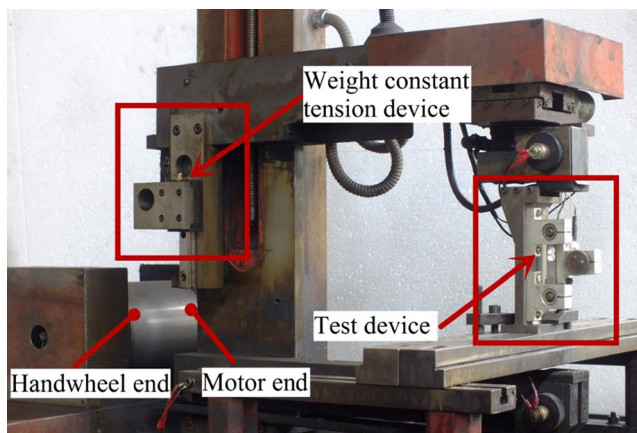
electrically conductive materials with precise, complex, and irregular shapes in the automobile, aerospace, and electronics industries, which with a flexible metal wire as an electrode transforms electrical energy into thermal energy for removing materials [1–3]. And the WEDM machines can be categorized according to wire running speed, that is, high-speed WEDM (HSWEDM) machines and low-speed WEDM (LSWEDM) WEDM machines [4, 5]. The high-speed WEDM machines were originally developed in China, and they exhibit high performance to price ratio and good capability to process large and thick workpieces [6]. The wire electrode used in HSWE DM is reciprocated for use and its speed is 8–12 m/s, which is significantly higher than that in LSWEDM [4]. In the WEDM process, the wire electrode is always pushed away from the workpiece by the discharging force [7, 8], thus resulting in a form and position error that changes with wire tension [9]. So wire tension strongly influences the dynamic position accuracy of the wire electrode, especially the non-even wire tension problem in the HSWEDM process. That is, the tensions of the wire electrode at both ends of a wire-winding cylinder become inconsistent after running a certain period [10]. This problem can cause a short circuit, an open circuit, and a series of abnormal discharge phenomena, which, in turn, can affect the machining accuracy and surface quality of a workpiece [11]. For this reason, it is necessary to investigate further the regularities of the wire tension change in HSWEDM and find out some effective methods to solve non-even wire tension problem to improve the machining precision and cutting stability. Liu et al. and Li et al. [10, 11] have studied the effect of power parameters and dielectric

✉ Liu Zhidong
liutim@nuaa.edu.cn

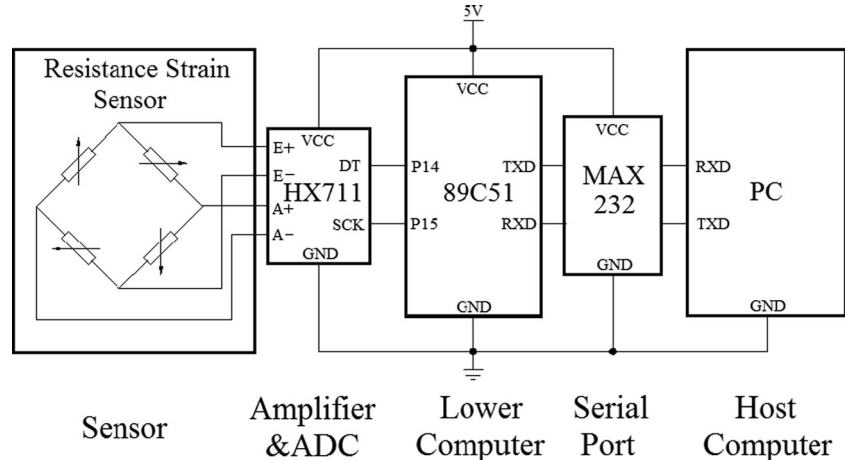
¹ College of Mechanical and Electrical Engineering, Nanjing University of Aeronautics and Astronautics, Nanjing 210016, China

Table 1 Experimental conditions

Item	Parameter
Wire electrode	Length=250 m, $\phi=0.18$ mm
Wire speed	12 m/s
Upper and lower guide wheel distance	300 mm
Initial wire tension	8 N

**Fig. 1** Weight constant tension device and tension test device

fluid on the wire tension change in HSWEDM; thus, this paper will study mainly the effect of wire-winding mechanism on the wire tension change. Then, simulation analysis is performed to redesign the wire-winding mechanism and conduct a series of comparison experiments.

Fig. 2 Principle diagram of tension test device

2 Cause analysis of wire tension change

2.1 Experimental conditions and results

The experiment was conducted in a typical HSWEDM machine, and the conditions are listed in Table 1. First, this paper used the weight constant tension device (Fig. 1) to generate an initial tension for the wire electrode and applied the test device to sample the wire tension waveform. Then, the wire electrode is pulled away from the weight constant tension device until the wire tension is stable.

The principle of the tension test device is shown in Fig. 2. It uses a resistance strain sensor to convert wire tension into electrical signal, which in turn is amplified and converted into digital signal with the HX711 chip. And the digital signal is transmitted from the lower computer to the host computer by the MAX232 chip; thereby, the sampling data of wire tension can be displayed real-timely and stored with the LabVIEW software. As shown in Fig. 3, the initial wire tension can be measured at approximately 8 N.

Tension waveforms are shown in Figs. 4 and 5 after running 10 and 100 min, respectively. The lower waveform in Figs. 4 and 5 is wire speed.

The above two figures show that the tension waveform exhibited peaks when changing moving direction. With increased running time, one peak becomes concave, whereas the other becomes convex. And tension waveform of positive moving (wire electrode moving from top to bottom) and negative moving (wire electrode moving from bottom to top) is not symmetrical but staggering.

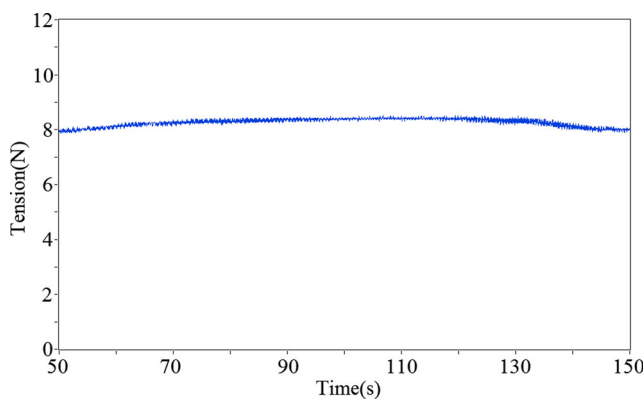


Fig. 3 The initial wire tension

2.2 Analysis of wire tension change

Figure 6 depicts the schematic diagram of the wire-winding mechanism in HSWEDM. When the wire-winding cylinder begins to positive accelerate, the wire electrode needs not only to overcome the friction with the conductive block (ignoring the friction between the wire electrode and the guide wheel) but also to overcome the inertial force (in the opposite direction of the wire electrode movement) that is brought about by guide wheels during acceleration. When the wire-winding cylinder is in uniform motion, the wire electrode just needs to overcome the friction with the conductive block. When the wire-winding cylinder begins to positive decelerate, guide wheels will give the wire electrode an inertial force of deceleration (in the same direction of wire electrode movement). The same phenomenon happens with negative moving.

As shown in Fig. 7, if a motor that is in uniform motion is stopped, the tension waveform will rise. If the motor is then run again, the tension waveform will

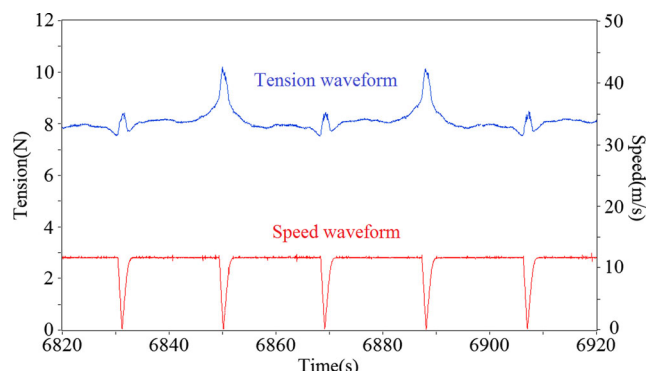


Fig. 5 Wire tension after running for 100 min

immediately return to normal. After the moving direction is changed, the tension waveform will present a peak in the corresponding position of the wire-winding cylinder where the motor stopped. This phenomenon shows that the peak of the tension waveform is generated by inertial force brought about by guide wheels.

Figure 8a, b shows the tension waveforms when the protection block is pressed and loosened, respectively. Comparison of the figures suggests that the symmetry of the tension waveform is associated with the protection block. The formula of the friction between the conductive block and the wire electrode is as follows:

$$F = (e^{\mu\theta} - 1) \cdot T$$

Here, F is the friction between the conductive block and the wire electrode, T is the wire tension, μ is the friction coefficient between the conductive block and the wire electrode, and θ is the corresponding central

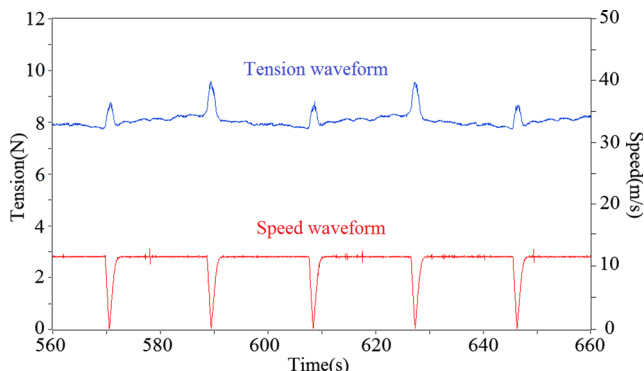


Fig. 4 Wire tension after running for 10 min

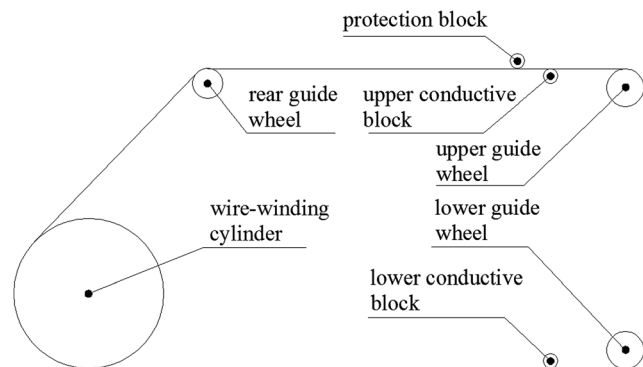


Fig. 6 Schematic diagram of wire-winding mechanism

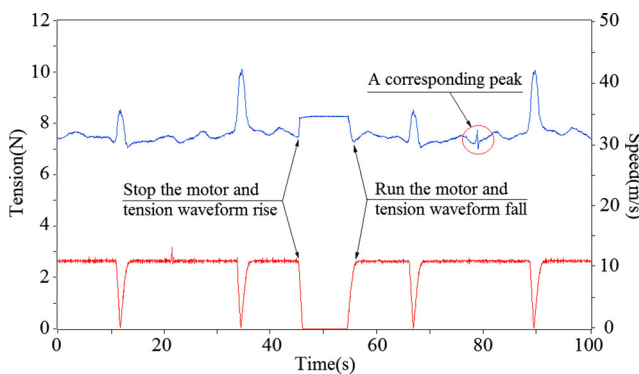


Fig. 7 Tension waveform when stopping and running the motor

angle between the conductive block and the wire electrode.

For ease of discussion and accounting, this paper referred to $(e^{\mu\theta}-1)$ as friction exponent (f). As shown in Fig. 8a, the tension waveform of positive moving will be wholly greater than that of negative moving when the friction exponent of the upper guide frame (f_{up}) is greater than the lower one (f_{low}). On the contrary, the tension waveform of positive moving will be wholly less than that of negative moving (Fig. 8b). Therefore, f_{up} and f_{low} can determine the tension waveform symmetry of positive and negative moving.

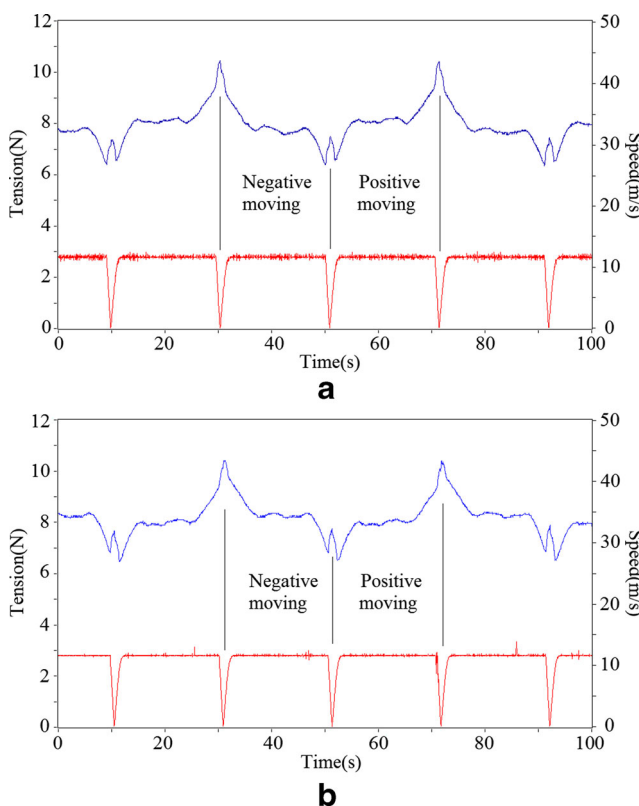


Fig. 8 **a** Tension waveform when pressing protection block. **b** Tension waveform when loosening protection block

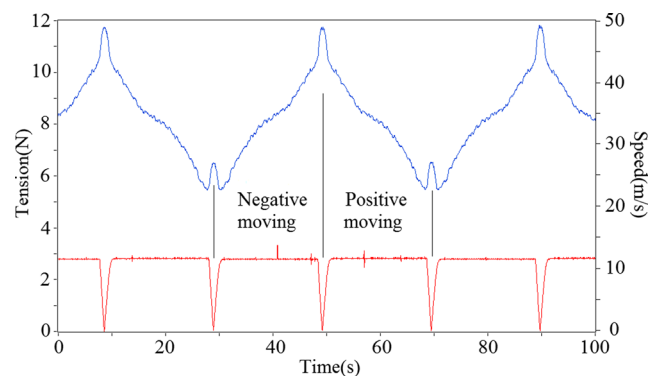


Fig. 9 Tension waveform when f_{up} is close to f_{low}

In addition, we found that f_{up} and f_{low} can determine the change trend of non-even wire tension in some condition. As shown in Fig. 9, non-even wire tension still appears when f_{up} is close to f_{low} . Analysis suggests that although f_{up} is close to f_{low} , the wire-winding mechanism is not completely symmetric (such as the number and the installation location of guide wheels on the upper and lower guide frames). Thus, the wire-winding mechanism exists as an asymmetric coefficient (f). As shown in Fig. 10a, the wire tension will present the change trend of “the motor end loose and the handwheel end tight.”

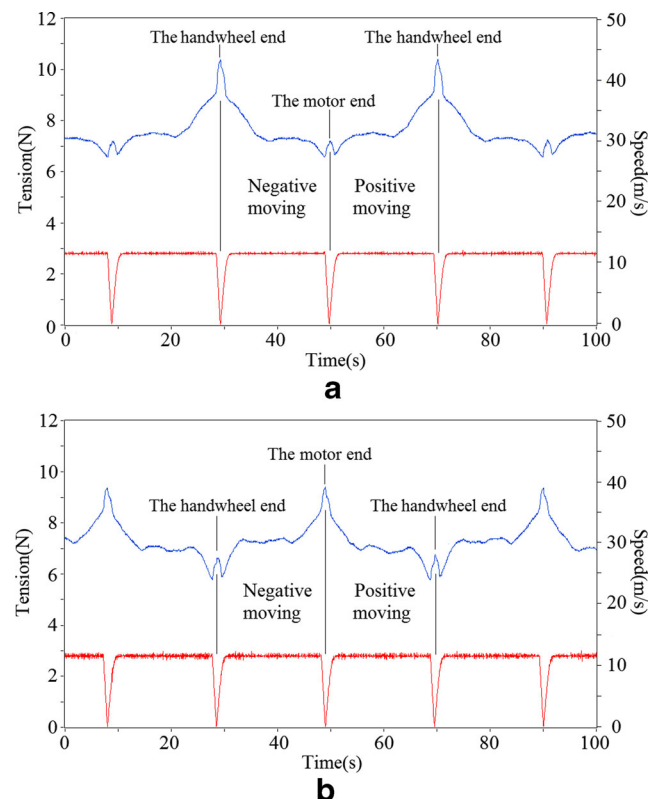


Fig. 10 **a** Change trend of “the motor end loose and the handwheel end tight.” **b** Change trend of “the motor end tight and the handwheel end loose”

Fig. 11 Interface of wire tension simulation

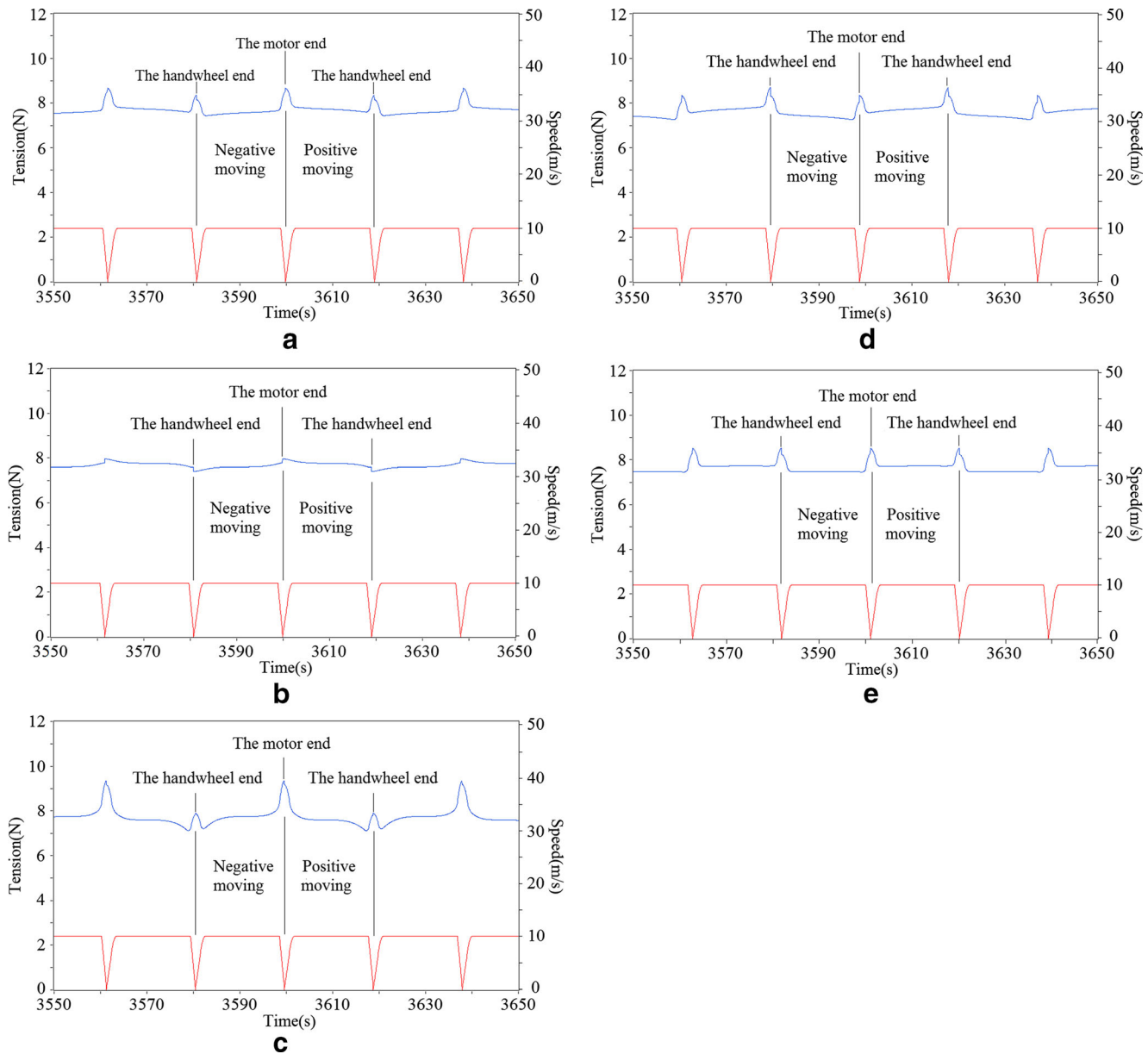
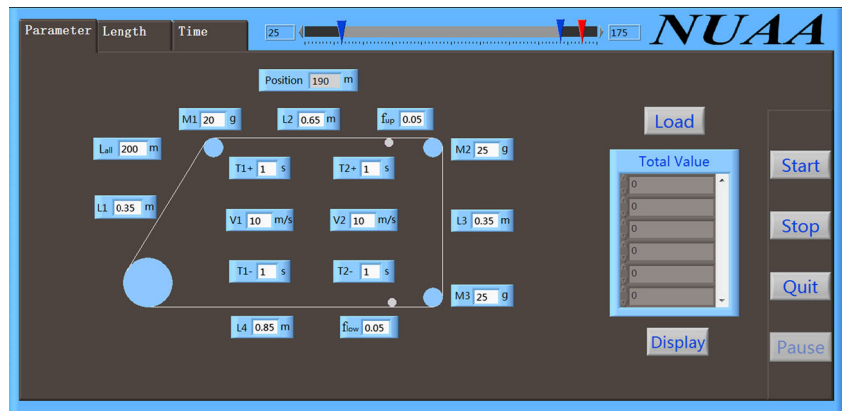
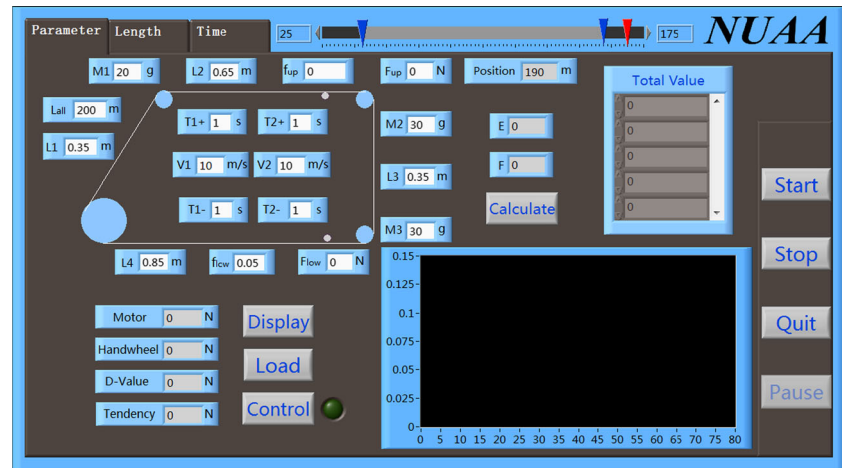


Fig. 12 **a** Simulation waveform ($f_{up}=0.05$ and $f_{low}=0.03$). **b** Simulation waveform ($m_1=m_2=m_3=0$). **c** Simulation waveform ($f_{up}=0.03$ and $f_{low}=0.05$). **d** Simulation waveform ($f_{up}=0.07$ and $f_{low}=0.03$). **e** Simulation waveform ($f_{up}=0.06$ and $f_{low}=0.03$)

Fig. 13 Interface of wire tension control simulation



handwheel end tight" when $f_{up} - f_{low} > f$. On the contrary, it will present the change trend of "the motor end tight and the handwheel end loose" when $f_{up} - f_{low} < f$ (Fig. 10b).

Moreover, a more asymmetric wire-winding mechanism corresponds to a larger asymmetric coefficient (f), and then the condition of $f_{up} - f_{low} < f$ appears more easily. Consequently, for the HSWEDM with such wire-winding mechanism, wire tension is usually tight at the motor end and loose at the handwheel end [11].

3 Simulation of wire tension change

A comparison of Figs. 4 and 5 demonstrates that with increasing running time, the wire tension change also increases and develops toward the trend of non-even wire tension. However, no parameters were changed in the test process. This phenomenon suggests that wire tension has a "potential" self-adjustment process within the wire-winding mechanism, and this process is unique to HSWEDM.

Table 2 Simulation parameters

Item	Parameter	Item	Parameter
L	200 m	f_{low}	0.03
L_1	0.3 m	t_1^+	1 s
L_2	0.65 m	V_1	10 m/s
L_3	0.3 m	t_1^-	1 s
L_4	0.85 m	t_2^+	1 s
m_1	20 g	V_2	10 m/s
m_2	25 g	t_2^-	1 s
m_3	25 g	T_0	8 N
f_{up}	0.05		

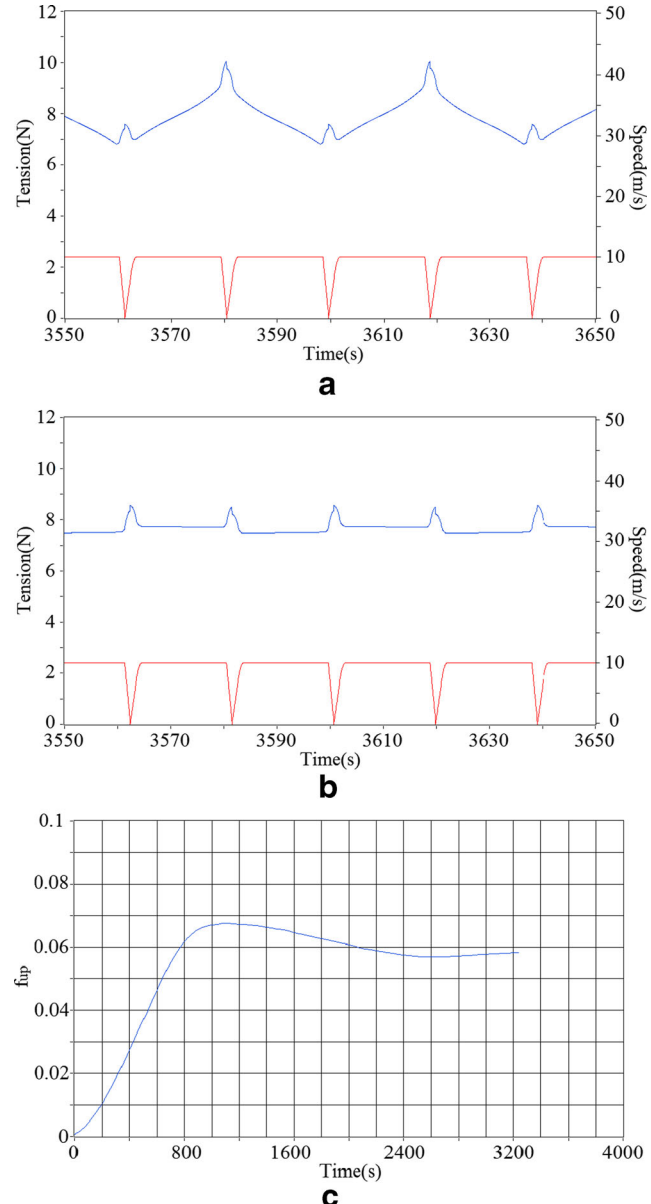


Fig. 14 **a** Simulation waveform without control. **b** Simulation waveform with control. **c** Control waveform of f_{up}

For further analysis of the relationship between self-adjustment process and wire tension change, this paper utilized the LabVIEW Software to establish the corresponding simulation model of wire tension (Fig. 11), and the simulation waveforms are shown in Fig. 12.

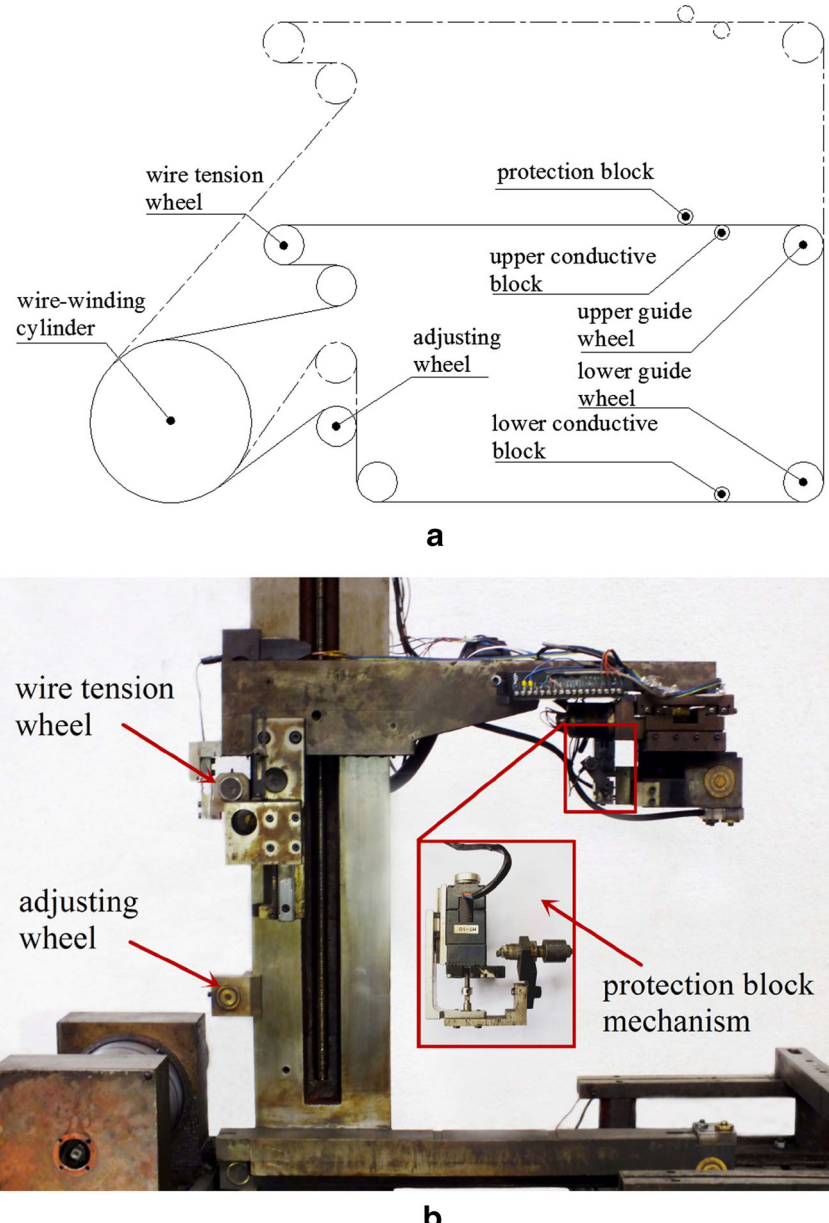
Here, L is the total length of the wire electrode, L_1 is the length of wire electrode between the wire-winding cylinder and the rear guide wheel, L_2 is the length of the wire electrode between the rear and upper guide wheels, L_3 is the length of the wire electrode between the upper and lower guide wheels, L_4 is the length of the wire electrode between the lower guide wheel and the wire-winding cylinder, m_1 is the quality of the rear

guide wheel shaft, m_2 is the quality of the upper guide wheel shaft, m_3 is the quality of the lower guide wheel shaft, t_{1+} is the positive acceleration time, V_1 is the positive wire speed, t_{1-} is the positive deceleration time, t_{2+} is the negative acceleration time, V_2 is the negative wire speed, t_{2-} is the negative deceleration time, and T_0 is the initial wire tension.

The simulation parameters of Fig. 12a are provided in Table 2. Wire tension presents the change trend of “the motor end tight and the handwheel end loose.” That is, $f_{up} - f_{low} < f$.

The simulation parameters of Fig. 12b are the same as those of Fig. 12a, except for $m_1 = m_2 = m_3 = 0$. A comparison of Fig. 12a and b revealed that the peak of

Fig. 15 **a** Schematic diagram of redesigned wire-winding mechanism. **b** Photo of redesigned wire-winding mechanism



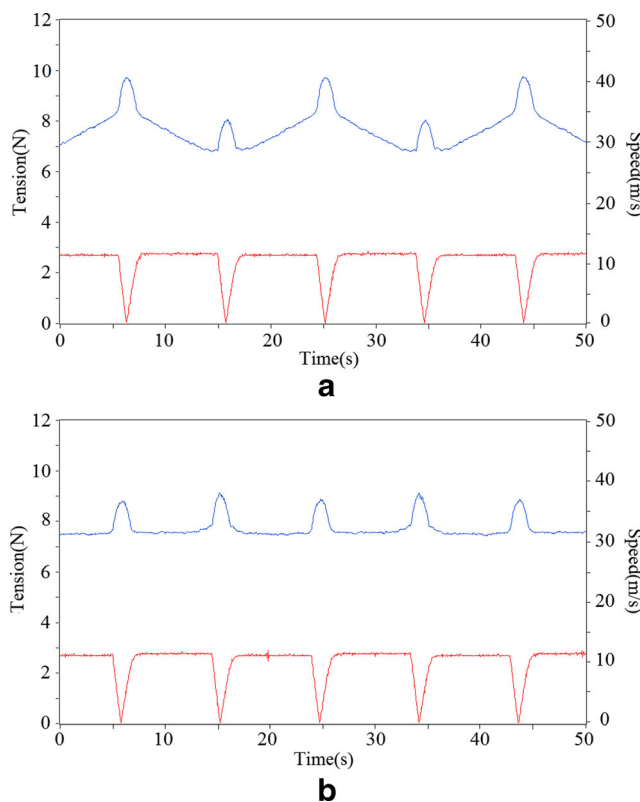


Fig. 16 **a** Tension waveform on original mechanism. **b** Tension waveform on redesigned mechanism

Table 3 Experimental conditions of large thickness cutting

Item	Parameter
Power parameters	$T_{on}=64 \mu s$, $T_{off}=10$, power amplifier tube=5
Dielectric fluid	JR1A (ratio with water is 1:20)
Wire electrode	Length=300 m, $\phi=0.18$ mm
Workpiece material	Die steel Cr12
Workpiece size	$6 \times 4 \times 400$ mm

tension waveform has changed markedly. Thus, the peak of tension waveform is assumed to be generated by the inertial force brought about by guide wheels.

The simulation parameters of Fig. 12c are the same as those of Fig. 12a, except for $f_{up}=0.03$ and $f_{low}=0.05$. Combining Fig. 8a and b and then comparing them to Fig. 12a, c verifies that f_{up} and f_{low} determine the tension waveform symmetry of positive and negative moving.

The simulation parameters of Fig. 12d are the same as those of Fig. 12a, except for $f_{up}=0.07$ and $f_{low}=0.03$. Wire tension presents the change trend of “the motor end loose and the handwheel end tight.” That is, $f_{up}-f_{low}>f$.

The simulation parameters of Fig. 12e are the same as those of Fig. 12a, except for $f_{up}=0.06$ and $f_{low}=0.03$. In Fig. 12e, wire tension does not present a clear change trend of non-even wire tension. The reason is that $f_{up}-f_{low}$ is close to f . Combining Fig. 12a and d verifies that f_{up} and f_{low} also determine the change trend of non-even wire tension under some conditions.

4 Wire tension control simulation and wire-winding mechanism redesign

On the basis of cause analysis and model simulations, the basic problem of wire tension change is caused by the symmetry of wire-winding mechanism in HSWEDM. By using the law that f_{low} and f_{up} determine the change trend of non-even wire tension under some condition, the relationship between $f_{up}-f_{low}$ and f can be adjusted to keep wire tension stable.

4.1 Wire tension control simulation

To further verify its feasibility, this paper added a control unit of f_{up} on the basis of the wire tension simulation model (Fig. 13).

All parameters in Table 2 (except for $f_{up}=0$) are taken to the above simulation model, and the simulation waveforms are shown in Fig. 14.

In Fig. 14a, f_{up} is out of control (i.e., always 0), and the simulated waveform presents an obvious non-even wire tension.

In Fig. 14b, the simulation waveform with control is similar to that in Fig. 12e. In Fig. 14c, f_{up} is close to 0.06, which is

Table 4 Experimental results

Wire-winding mechanism	Tension waveform	Discharge waveform	Processing time
Original mechanism	Present obvious phenomenon of non-even wire tension (Fig. 17)	Normal discharge at the handwheel end (Fig. 18a) and short circuit at the motor end (Fig. 18b)	Increasing constantly (Fig. 21)
Redesigned mechanism	Keep stable basically (Fig. 19)	Normal discharge at both ends (Fig. 20)	Increasing slowly (Fig. 21)

consistent with Fig. 12e, thus verifying the feasibility of this control method.

4.2 Wire-winding mechanism redesign

To combine with practical application demands, this paper redesigned the wire-winding mechanism (Fig. 15). Thus, the relationship between f_{up} – f_{low} and f can be adjusted by controlling an adjusting wheel and protection block.

Under the same conditions, the original wire-winding mechanism (Fig. 6) and the redesigned one were utilized to perform comparison experiments regarding wire tension. The results are shown in Fig. 16.

A comparison of Fig. 16a and b revealed that the redesigned wire-winding mechanism can keep wire tension stable, and the control effect is consistent with the simulation result.

In addition, the existing weight or closed-loop constant tension device [12, 13] did not consider the loss of the wire electrode in the machining process, and it just kept the wire electrode at a constant tension, indicating that the wire electrode could easily snap when its diameter becomes fine [14]. The redesigned wire-winding mechanism in this paper cannot only keep wire tension stable but also realizes that wire tension will gradually decrease as the diameter of the wire electrode becomes fine. Thus, the probability of the wire electrode to snap is greatly minimized.

5 Process comparison experiments

5.1 Large thickness cutting comparison experiment

This paper used the original wire-winding mechanism and redesigned one to conduct a large thickness cutting comparison experiment. The experimental conditions are

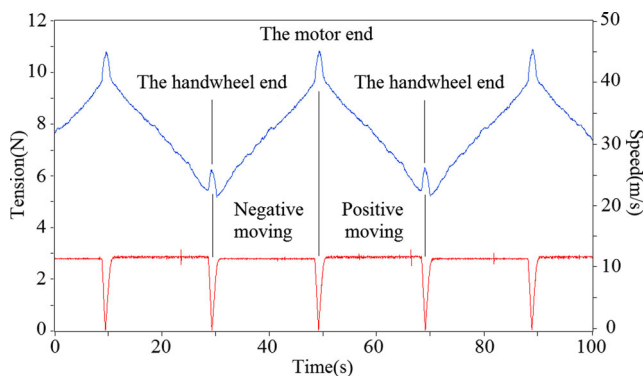


Fig. 17 Tension waveform of large thickness cutting on original wire-winding mechanism

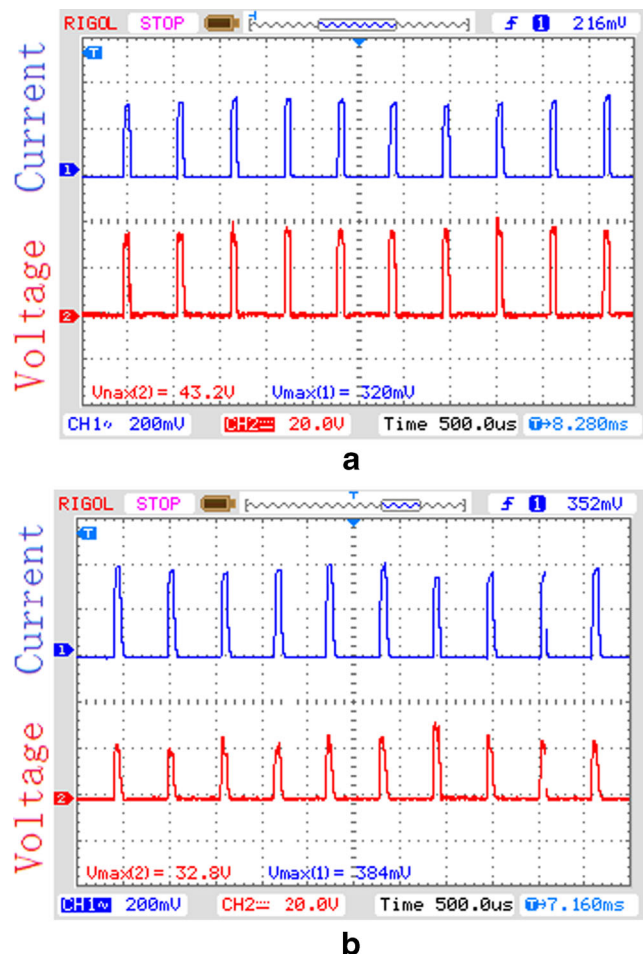


Fig. 18 **a** Discharge waveform at the handwheel end. **b** Discharge waveform at the motor end

shown in Table 3, and the experimental results are shown in Table 4 (Figs. 17, 18, 19, and 20).

In Fig. 21, as the phenomenon of non-even wire tension became obvious gradually on original wire-winding mechanism, the probability of short circuit will increase accordingly, causing processing time to increase

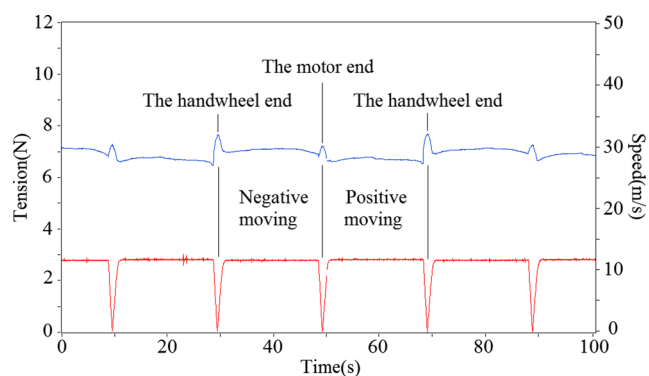


Fig. 19 Tension waveform of large thickness cutting on redesigned wire-winding mechanism

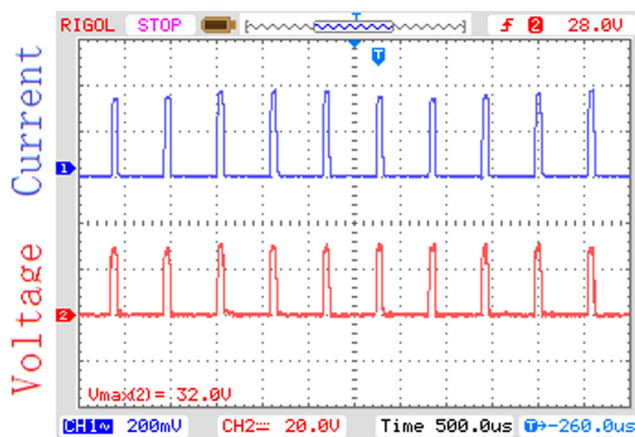


Fig. 20 Discharge waveform at both ends

constantly. However, there was not an obvious phenomenon of non-even wire tension and short circuit on the redesigned wire-winding mechanism, causing the processing time to increase more gradually slowly. Compared with that of the original wire-winding mechanism, the average cutting efficiency of the redesigned device was improved by 8 %.

Therefore, the redesigned wire-winding mechanism can effectively improve the cutting stability and efficiency in large thickness cutting processes.

5.2 Multi-cutting comparison experiment

This paper used the original wire-winding mechanism and redesigned one to carry out multi-cutting comparison experiment. The experimental conditions are shown in Table 5, and the maximum dimension error of workpiece is shown in Fig. 22. The findings show that the redesigned wire-winding mechanism is helpful in improving the consistency of workpiece dimension in multi-cutting processes. Particularly on the original wire-winding mechanism, the maximum dimension error

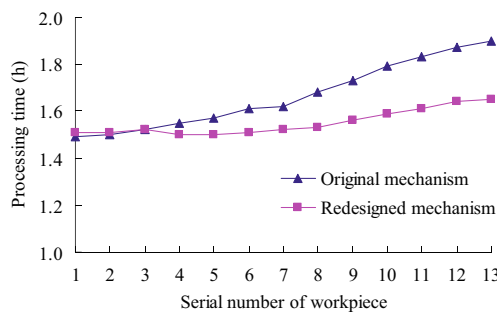


Fig. 21 Processing time comparison of the two mechanisms

Table 5 Experimental conditions of multi-cutting

Item	Parameter
Power parameters	1. Ton=40 μ s, Toff=8, power amplifier tube=11 2. Ton=10 μ s, Toff=14, power amplifier tube=6 3. Ton=1.6 μ s, Toff=8, power amplifier tube=11
Dielectric fluid	JR1A (ratio with water is 1:20)
Wire electrode	Length=300 m, $\phi=0.18$ mm
Workpiece material	Die steel Cr12
Workpiece size	Octagonal column (distance across flats=12 mm, thickness=40 mm)

continued to increase, whereas on the redesigned wire-winding mechanism, the maximum dimension error was maintained at approximately 6 μ m.

6 Conclusions

1. The cause analysis and model simulations showed that the symmetry of wire-winding mechanism and the resistance to wire electrode on the upper and lower guide frames are the basic reasons for non-even wire tension.
2. The redesigned wire-winding mechanism in this paper cannot only keep wire tension stable but can also diminish the probability of wire electrode snapping. In addition, it can effectively improve cutting stability and efficiency in large thickness cutting processes, as well as the consistency of workpiece dimension in multi-cutting processes.

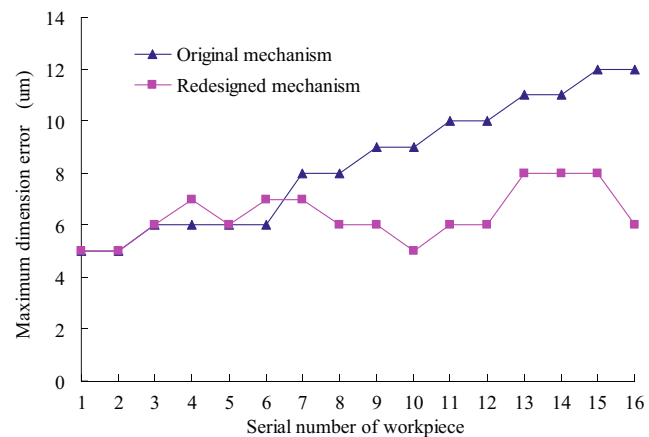


Fig. 22 Maximum dimension error of workpiece

References

1. Gauri SK, Chakraborty S (2010) A study on the performance of some multi-response optimisation methods for WEDM processes. *Int J Adv Manuf Technol* 49:155–166
2. Lee WM, Liao YS (2007) Adaptive control of the WEDM process using a self-tuning fuzzy logic algorithm with grey prediction. *Int J Adv Manuf Technol* 34(5–6):527–537
3. Ho KH, Newman ST, Rahimifard S, Allen RD (2004) State of the art in wire electrical discharge machining (WEDM). *Int J Mach Tools Manuf* 44(12–13):1247–1259
4. Hou PJ, Yf G, Shao DX, Li ZF, Wureli Y, Tang L (2014) Influence of open-circuit voltage on high-speed wire electrical discharge machining of insulating zirconia. *Int J Adv Manuf Technol* 73:229–239
5. Fan YS, Bai JC, Li CJ, Xu W (2013) Research on precision pulse power technology of WEDM. *Procedia CIRP* 6:268–274
6. Liu ZD, Gao CS (2011) Electrical discharge machining technology and application. China Machine Press, Beijing
7. Puri AB, Bhattacharyya B (2003) An analysis and optimisation of the geometrical inaccuracy due to wire lag phenomenon in WEDM. *Int J Mach Tools Manuf* 43(2):151–159
8. Fan SY, Zhang QJ, Chen HW, Zeng WX (2013) Nonlinear dynamics analysis of multi-cutting wire electrode in WEDM-HS subjected to working fluid considering the effect of debris. *J Mech Sci Technol* 27(12):3595–3605
9. Li MQ, Li MH, Xu GY (2005) Study on the variations of form and position of the wire electrode in WEDM-HS. *Int J Adv Manuf Technol* 25(9–10):929–934
10. Liu ZD, Li XF, Li MM (2013) Research on non-even wire tension in HSWEDM. Proceedings of the 15th National Conference on non-traditional machining 211–217
11. Li LL, Liu ZD, Li XF, Li MM (2014) Non-even wire tension in high-speed wire electrical discharge machining. *Int J Adv Manuf Technol* 78(1–4):503–510
12. Yang JJ, Wu FM, Rao L et al (2006) Study on the constant tension mechanism for HS-WEDM. *Mod Mach* 3:95–96
13. Jiang YC, Ren FJ (2008) Constant tension control system of wire tool in WEDM-HS based on PMAC. *China Mech Eng* 3:1920–1924
14. Wang ZW, Wang BX (2013) Study on the wire tension system of HS-WEDM. *Electromachining Mould* 5:63–65